Inhomogeneous broadening of the Ce^{3+} luminescence in $CaYAlO_4$

1996 J. Phys.: Condens. Matter 8 3505

(http://iopscience.iop.org/0953-8984/8/19/024)

J. Phys.: Condens. Matter **8** (1996) 3505–3512. Printed in the UK

Inhomogeneous broadening of the Ce^{3+} luminescence in $CaYAlO_4$

N Kodama†‖, M Yamaga‡ and B Henderson§

† Tosoh Corporation, Hayakawa, Ayase 252, Japan

‡ Department of Physics, Faculty of General Education, Gifu University, Gifu 501-11, Japan

§ Department of Physics and Applied Physics, University of Strathclyde, Glasgow G1 1XN, UK

Received 18 December 1995

Abstract. Five absorption bands with peaks at $\leqslant$210 nm, 246 nm, 284 nm, 296 nm, and 368 nm were observed at room temperature for Ce-doped $CaYAlO_4$ (CYA) crystals grown in a reducing atmosphere. Excitation at wavelengths below ∼400 nm of Ce:CYA crystals produces a broad luminescence band with a peak at ∼485 nm. The excitation spectrum of the luminescence detected at a fixed wavelength of 485 nm is very similar to the absorption spectrum. The ultraviolet absorption and visible luminescence are due to the $4f^1 \leftrightarrow 5d^1$ transitions of Ce^{3+} ions in CYA. The linear dependence of the luminescence peak energy on the excitation energy shows that the luminescence is inhomogeneously broadened by a random distribution of Ca^{2+} and Y^{3+} ions in the disordered CYA lattice.

1. Introduction

Optical transitions between $4f^n$ electronic configurations in most trivalent rare-earth ions (Nd^{3+}, Er^{3+}, Ho^{3+} etc) give rise to narrow fluorescence lines in the presence of very weak electron–phonon coupling. Generally, the 5d energy levels of these ions are above the ultraviolet (UV) region. In contrast, the optical transitions of Ce^{3+} ions in some crystals are observed in the UV or visible regions because the 5d energy levels of Ce^{3+} ions are considerably lower in energy than those of other trivalent rare-earth ions. Laser operation in the UV region near 0.3 μm for the use of the $4f^1 \leftrightarrow 5d^1$ transition has been reported for Ce^{3+}-doped $LiYF_4$ and LaF_3 [1, 2].

The change in the energy levels of Ce^{3+} ions from one host to another is expected because the 5d energy levels are strongly affected by the crystal field. The crystal field increases with decreasing distance between Ce^{3+} and ligand ions and with increasing valency ($F^- \rightarrow O^{2-}$) and number of ligand ions. Ce^{3+}-doped $Y_3Al_5O_{12}$ crystals show the absorption and luminescence in the visible region. The $5d^1 \rightarrow 4f^1$ luminescence band peaks at 570 nm with a near-unity quantum efficiency at room temperature. Nevertheless, the lasing efficiency is very poor due to excited-state absorption, in which the pump radiation produces optical transitions from the lowest 5d excited state to the host conduction band [3]. Since Ce^{3+}-doped crystals have considerable potential as tunable laser gain media it is important to further study the effects of different crystal fields on the 5d excited energy levels.

In earlier papers [4–6], the authors have discussed the properties of Ti^{3+}, V^{4+} and Cr^{3+} in $CaYAlO_4$ (CYA). Such crystals have a distribution of the crystal field caused

‖ Present address: Department of Chemistry, Faculty of Education, Akita University, Akita 010, Japan.

0953-8984/96/193505+08$19.50

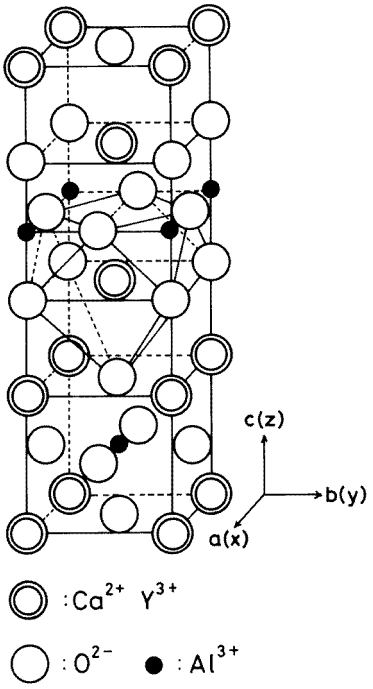

Figure 1. Crystal structure of $CaYAlO_4$

by *substitutional disorder* of the Ca^{2+}/Y^{3+} sites in the CYA lattice. We have extended these studies to CYA crystals doped with Ce^{3+} ions. The crystal field of Ce^{3+} in CYA is intermediate between those of $LiYF_4$ and $Y_3Al_5O_{12}$. This paper describes the crystal growth of Ce^{3+}-doped CYA, and absorption, luminescence, and excitation spectra in this disordered host lattice.

2. Crystal structure and growth

Figure 1 shows the structure of $CaYAlO_4$ (CYA) with space group $I4/mmm$ (D_{4h}^{17}). The lattice constants are $a = b = 3.6451$ Å and $c = 11.8743$ Å [7, 8]. Ca^{2+} and Y^{3+} ions are distributed at random keeping the composition ratio of 1:1. The Ca^{2+}/Y^{3+} ions are surrounded by nine nearest-neighbour oxygen ligand ions. The symmetry is C_{4v}. Site occupancy is expected to be determined largely by considerations of ionic size. In consequence, Ce^{3+} ions are expected to preferentially occupy Ca^{2+}/Y^{3+} sites because the radius (1.11 Å) of Ce^{3+} is closer to those of Ca^{2+} (0.99 Å) and Y^{3+} (0.93 Å), and much larger than that of Al^{3+} (0.51 Å).

Single crystals were grown by the Czochralski technique from melts prepared in iridium crucibles with high-purity components $CaCO_3$(5N):Y_2O_3(5N):Al_2O_3(5N) = 2:1:1. CYA crystals doped with CeO_2 at a concentration of 0.5 mol% were grown in a reducing atmosphere (1% H_2:99% Ar) in order to convert Ce^{4+} to Ce^{3+}, or in an inert (Ar gas) atmosphere. The resulting boules were cut and polished into samples with approximate dimensions $4 \times 4 \times 1$ mm^3 for use in the optical measurements. The cut faces were normal to the *a*, *b* and *c* axes of the crystal. Other samples were annealed in reducing (5% H_2:95% Ar) or oxidizing (air) atmospheres at 1500 °C for 20 hours to examine changes in the valence state of the Ce impurity.

3. Experimental results

3.1. Absorption spectra

Optical absorption spectra were measured at room temperature using a dual-beam spectrophotometer. The polarization was measured by inserting a Glan–Thompson prism in the sample beam of the spectrophotometer and rotating it. The absorption spectra for the pure as-grown CYA crystals were reported in the previous paper [4]. The colour of such crystals is light brown, with an absorption coefficient of less than 0.2 cm^{-1} above 600 nm. With decreasing wavelengths from 600 nm, the absorption increases gradually: a broad band with peak at 420 nm is observed, of which the absorption coefficient is about 1 cm^{-1} and about 2 cm^{-1} at 300 nm.

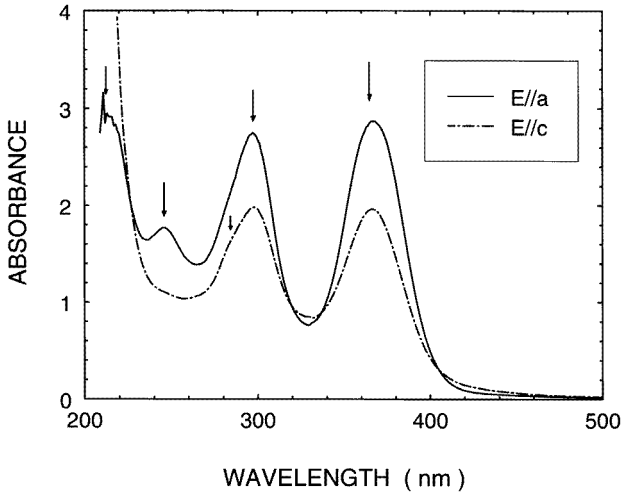

Figure 2. Polarized absorption spectra of the Ce:CYA crystal measured at room temperature. The $\boldsymbol{E}$-vectors of the light are parallel to the *a* and *c* axes.

The as-grown Ce:CYA crystals absorb fairly strongly in the UV region, the resulting crystal being light blue–green in colour. Figure 2 shows polarized absorption spectra. The 296 nm and 368 nm absorption bands are polarized along the *a* (*b*) axis more strongly than along the *c* axis. The polarization in the range below 220 nm suggests a peak at $\leqslant$210 nm. The 246 nm band is strongly polarized along the *a* axis and the intensity ($\boldsymbol{E} \parallel \boldsymbol{c}$) is negligibly weak. These polarized absorption spectra show clearly five bands including a weak band at 284 nm due to the Ce impurities in CYA, denoted by arrows in figure 2. The large absorption coefficient is caused by the 4f and 5d wavefunctions, so optical transitions are parity allowed and of electric dipole nature. This absorption spectrum is very similar to those observed in the UV region in other Ce^{3+}-doped oxide and fluoride crystals [9, 10], which were similarly attributed to the $4f^1 \rightarrow 5d^1$ transition of Ce^{3+} ions in CYA.

3.2. Luminescence and excitation spectra

Luminescence and excitation spectra were measured at room temperature using a HITACHI F-4500 Fluorescence Spectrophotometer. UV excitation in the range 340–420 nm at 300 K of the as-grown Ce:CYA sample produces the broad luminescence band with a peak at

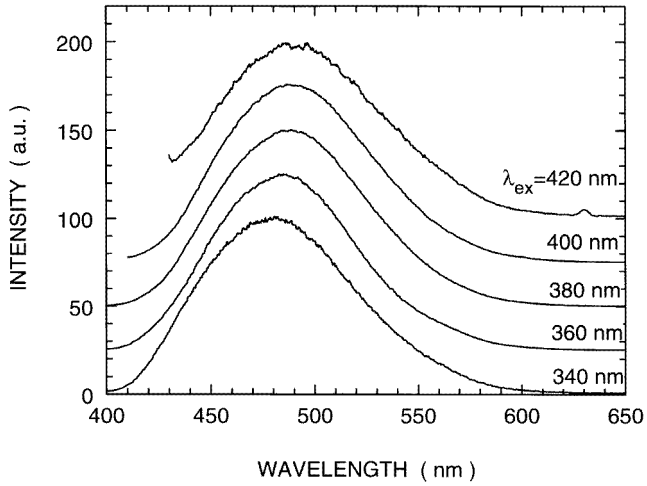

Figure 3. Luminescence spectra of Ce^{3+} in the Ce:CYA crystal excited at different wavelengths and measured at room temperature.

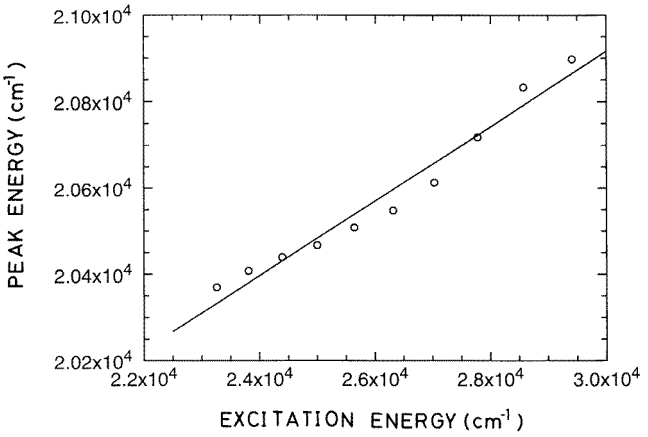

Figure 4. The relationship between luminescence peak energy and excitation energy for the Ce:CYA crystal. The straight line was calculated by the method of least squares. The gradient is 0.09.

around 485 nm shown in figure 3. With increasing excitation wavelengths, the peaks of the luminescence bands shift to longer wavelength. Figure 4 shows the linear dependence of the luminescence peak energy on the excitation energy. The slope of the straight line calculated by the method of least squares is 0.09. This value is slightly smaller than that (0.25) observed for V^{4+}:CYA [5].

The excitation spectra of the luminescence shown in figure 5 were detected at different fixed wavelengths in the range 430–550 nm. They comprise an intense band with a peak at ∼385 nm and two weak bands with peaks at ∼250 nm and ∼295 nm. Although the peak wavelengths of the two weak excitation bands are coincident with those of the absorption bands in figure 2, the intense 385 nm excitation band is shifted to slightly longer

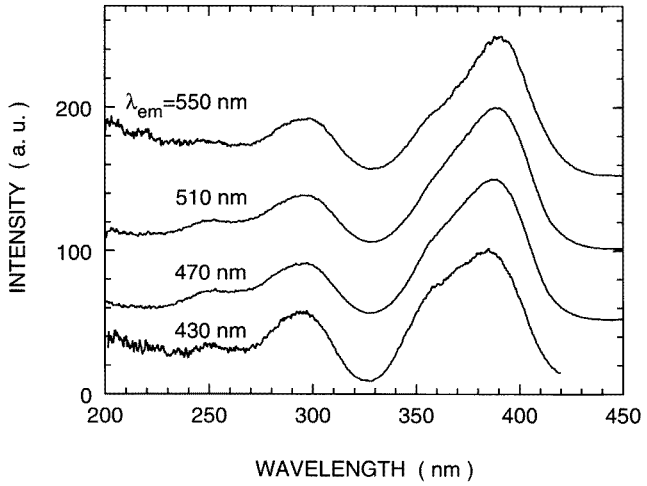

Figure 5. Excitation spectra of the luminescence detected at different fixed wavelengths measured at room temperature for the Ce:CYA crystal.

wavelength and is broadened somewhat compared with the 368 nm absorption band. The excitation spectrum is recorded as monitoring the luminescence intensity as a function of the wavelength of radiation absorbed by Ce^{3+} ions in the crystals. The radiation emitted under the UV excitation below 390 nm comes only from the surface, while that emitted under the excitation above 390 nm comes from the bulk sample. The strong absorption below 390 nm may reduce the luminescence intensity somewhat because of the scattering of the radiations on the surface. Then, the true peak wavelength of the excitation band is expected to be a little shorter than the observed peak wavelength. In addition, the peak shift of the excitation spectra to longer wavelength is very small as the detecting wavelengths of the luminescence increase as shown in figure 5.

The thermal treatment of the Ce:CYA crystals grown in a reducing atmosphere does not change the shape and the intensity of the luminescence compared with those for the as-grown samples. Although the Ce:CYA crystals grown in an inert atmosphere show strong absorption in the UV region, excitation below 400 nm produces no broad luminescence band similar to that in the Ce:CYA crystal grown in a reducing atmosphere. In consequence, the crystal growth in a reducing atmosphere is expected to convert Ce^{4+} to Ce^{3+} and the broad luminescence is assigned to be the $5d^1 \rightarrow 4f^1$ transition of Ce^{3+} ions in CYA.

4. Discussion

Ce^{3+} ions preferentially occupy Ca^{2+}/Y^{3+} sites, which are surrounded by nine nearest-neighbour oxygen ligand ions. The symmetry of Ce^{3+} is represented by C_{4v} in the absence of inversion symmetry. We consider the energy levels of Ce^{3+} in such a crystal field. The x, y, and z coordinates of the wavefunctions of Ce^{3+} are defined in figure 1. The electron configuration of the Ce^{3+} ground state is $4f^1$. Since the 4f electron is not strongly affected by the crystal field, the total angular momentum J-value is a good quantum number. The ^2F_J state of $4f^1$ ions is split by spin–orbit interaction into $^2F_{5/2}$ and $^2F_{7/2}$ levels separated by some 2000 cm^{-1} [10]. The excited electron $5d^1$ configuration is affected much more strongly by the crystal field than is $4f^1$. If the spin–orbit interaction is much larger than the crystal-field splitting of Ce^{3+}, J is also a good quantum number for the excited electron $5d^1$. The ^2D_J excited state is split into the $^2D_{3/2}$ and $^2D_{5/2}$ levels with the crystal-field

splitting being treated as a perturbation. However, if the crystal-field splitting is much larger than the spin–orbit interaction, then the excited 5d state is split into t_{2g} ($|xy\rangle$, $|yz\rangle$, $|zx\rangle$), and e_g ($|2z^2 - x^2 - y^2\rangle$, $|x^2 - y^2\rangle$) orbitals with the spin–orbit interaction being treated as a perturbation [11]. If these two different eigenfunctions include the higher-order perturbations, they are equivalent to each other. In the case of Ce:CYA, there is no evidence as to which effect is dominant: indeed, they are expected to be of comparable magnitude.

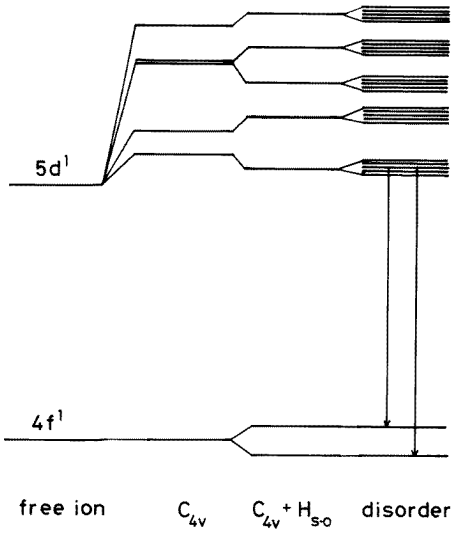

Figure 6. An energy diagram of Ce^{3+} in C_{4v} symmetry including spin–orbit interaction and disorder as perturbations.

Here we adopt a strong-crystal-field approach, where ligand ions are regarded as point charges. The lobes of the $|xy\rangle$, and $|yz\rangle$ ($|zx\rangle$) wavefunctions point towards the four ligand ions in the *ab* plane and toward two ligand ions in the *bc* (*ac*) plane, respectively. The lobe of $|2z^2-x^2-y^2\rangle$ extends towards a ligand ion on the *c* axis. On the other hand, the $|x^2-y^2\rangle$ wavefunction extends between ligand ions. According to a point charge theory, the energy levels of the 5d excited state are expected to be $|x^2 - y^2\rangle$, $|2z^2 - x^2 - y^2\rangle$, $|yz\rangle$ ($|zx\rangle$), and $|xy\rangle$ in order of increasing energy. When spin–orbit interaction is added to the Hamiltonian as a perturbation, the wavefunctions are mixed and the energy levels are shifted. Disorder introduces a distribution of crystal-field interaction, giving rise to the variation of the 5d energy levels. This energy situation is illustrated in figure 6. The wavefunctions of the 5d excited state will be discussed further in terms of the polarizations of the absorption and luminescence spectra and the symmetry of the ground state determined by the electron spin-resonance technique in a subsequent paper.

Assuming that absorption is to each of the five Kramers doublets of the 5d configuration split by the combined effects of crystal-field and spin–orbit interactions, then the luminescence occurs from the lowest excited energy level of 5d to the two $^2F_{5/2}$ and $^2F_{7/2}$ levels of the 4f ground state. Since the $5d^1 \rightarrow 4f^1$ transitions are parity and spin allowed, the decay time is tens of nanoseconds. As the 5d wavefunctions are somewhat extended toward ligands, a medium electron–phonon coupling is expected, resulting in a large Stokes shift energy $2S\bar{h}\omega$, where S is the Huang–Rhys factor and $\bar{h}\omega$ is the phonon energy, and a large linewidth of the Ce^{3+} luminescence [9, 10].

The Ce^{3+} luminescence spectrum in CYA has been decomposed into a sum of Gaussian bands of the form

$$I(\epsilon) = I_0 \exp\left(-(\epsilon - \epsilon_-)^2/(2\Gamma_{obs}^2)\right) \tag{1}$$

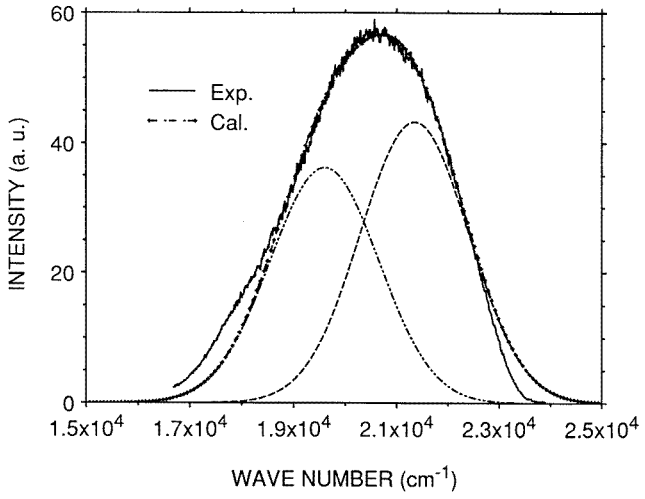

Figure 7. The decomposition of the luminescence spectrum into two Gaussians. The separation is 1750 cm^{-1}. The width is Γ = 1050 cm^{-1}.

where ϵ_- and Γ_{obs} are the peak energy and width of the luminescence band. The calculated curve, assuming values of $\epsilon_- = 19\,600$ and $21\,350$ cm^{-1} with $\Gamma_{obs} = 1050$ cm^{-1}, fits the observed spectrum in figure 7. The value (1750 cm^{-1}) of the energy separation is very close to those observed in Ce^{3+}:$Y_2Si_2O_7$ (1850 cm^{-1}) and Ce^{3+}:$LiYF_4$ (1950 cm^{-1}) [10]. The difference between the observed spectrum and the calculated curve at the lower and higher energies may be due to the assumption of a Gaussian band-shape. When the Huang–Rhys factor S is less than 6, the asymmetric line-shape is not a Gaussian, but a Pekarian [12].

The linear dependence of the peak energy of the Ce^{3+} luminescence on the excitation energy for the Ce:CYA crystals is the same as has been observed for V^{4+}:CYA crystals [5]. This observation suggests inhomogeneous broadening of the Ce^{3+} luminescence as a consequence of the random distribution of Ca^{2+}/Y^{3+} sites in different unit cells in CYA, which produces variations of the 5d excited energy levels as shown in figure 6.

We have extended the convolution method developed for V^{4+}:CYA [5] and Cr^{3+}:glasses [13, 14] to the Ce^{3+} luminescence in CYA crystals. The distribution function of the energy level, E, of the lowest excited state is assumed to be a Gaussian

$$P_e(E) = \frac{1}{\sqrt{2\pi}\gamma} \exp\left(-\frac{(E - E_0)^2}{2\gamma^2}\right) \tag{2}$$

where E_0 is the value of E with maximum probabilities, and γ is the width of the distribution.

The line-shape functions of the intrinsic absorption and luminescence spectra associated with the lowest excited state and the ground state are assumed to be Gaussians given by equation (1) with the replacement of Γ_{obs} by Γ. The line-shapes of the absorption and luminescence spectra of Ce^{3+} in CYA including the variation of the lowest excited-state energy level are also calculated as convolutions of the line-shape functions of the intrinsic spectra with the distribution function. The calculated line-shapes of the absorption and luminescence spectra are represented by Gaussians with peak energies of $\epsilon_+ = E_0$ and $\epsilon_- = E_0 - 2S\hbar\omega$, and the widths $\Gamma_{ab} = \sqrt{\Gamma^2 + \gamma^2}$ and $\Gamma_{em} = \sqrt{\Gamma^2 + \gamma'^2}$ where $\gamma'^2 = \Gamma^2\gamma^2/(\Gamma^2 + \gamma^2)$, respectively [13]. Here we assume that the variation of the Stokes shift energy $2S\hbar\omega$ is negligibly small compared with that of E.

The laser beam having a fixed excitation energy E_{ex} in the $4f^1 \rightarrow 5d^1$ absorption band excites various populations of Ce^{3+} ions in the different local crystal fields at the same time.

The distribution function of Ce^{3+} ions in the lowest excited state is given by the modified Gaussian with a parameter of E_{ex} [5, 13, 14]. The peak energy of the Gaussian line-shape of the luminescence excited with E_{ex} is given by

$$\epsilon_{-} = (E_0\Gamma^2 + E_{ex}\gamma^2)/(\Gamma^2 + \gamma^2) - 2S\bar{h}\omega. \tag{3}$$

The slope of ϵ_{-} versus E_{ex} which is equal to $\gamma^2/(\Gamma^2 + \gamma^2)$ is equal to 0.09 from the data in figure 4. Since the ratio of γ^2 to Γ^2 is rather small, $\simeq$0.1, the value of γ' is nearly equal to that of γ. The observed width of the luminescence band, Γ_{obs}, which is defined as Γ_{em} ($\simeq \Gamma_{ab}$), is obtained as 1050 cm^{-1} from figure 7. Then, the values of Γ and γ are estimated to be 1000 cm^{-1} and 320 cm^{-1}, respectively.

5. Conclusions

The energy levels of the 5d electronic excited state of Ce^{3+} in crystals are determined by the ion environment. The crystal field of Ce^{3+} in CYA is intermediate between those of $LiYF_4$ and $Y_3Al_5O_{12}$. The absorption of Ce^{3+} in CYA is observed in the UV region and the luminescence is in the green region. As there is random occupation of the Ca^{2+}/Y^{3+} sites in CYA crystals, the luminescence is inhomogeneously broadened. The inhomogeneous broadening is estimated from the relation of the luminescence peak energy to the excitation energy. The broadening enables the tuning range of a laser oscillation to broaden, although the gain will also be distributed over a larger bandwidth.

Acknowledgments

The present work was supported by a Grant-in-Aid for Scientific Research on Priority Areas 'New Development of Rare Earth Complexes' No 07230233 from The Ministry of Education, Science and Culture and by Joint Research Projects of the Japan Society for the Promotion of Science and the British Royal Society.

References

[1] Walling J C 1987 *Tunable Lasers* ed L F Mollenauer and J C White (Berlin: Springer) p 362
[2] Moulton P 1985 *Handbook* vol 5, ed M Bass and M H Stitch (Amsterdam: North-Holland) p 282
[3] Hamilton D S, Gayen S K, Pogatshnik G J, Ghen R D and Miniscalco W J 1989 *Phys. Rev.* B **39** 8807
[4] Yamaga M, Yosida T, Naitoh Y and Kodama N 1994 *J. Phys.: Condens. Matter* **6** 4381
[5] Yamaga M, Henderson B, Yosida T, Kodama N and Inoue Y 1995 *Phys. Rev.* B **51** 3438
[6] Yamaga M, Takeuchi H, Holliday K, Macfarlane P I, Henderson B, Inoue Y and Kodama N 1996 *Radiat. Eff. Defects Solids* **133–134** at press
[7] Oudalov J P, Daoudi A, Joubert J C, Flem G L and Hagenmuller P 1970 *Bull. Soc. Chim. Fr.* **10** 3408
[8] Shannon R D, Oswald R A, Parise J B, Chai B H T, Byszewski P, Pajaczkowska A and Sobolewski R 1992 *J. Solid State Chem.* **98** 90
[9] Blasse G 1979 *Handbook on the Physics and Chemistry of Rare Earths* vol 4, ed K A Gschneidner and L Eyring (Amsterdam: North-Holland) ch 34
[10] Blasse G and Grabmaier B C 1994 *Luminescent Materials* (Berlin: Springer)
[11] Sugano S, Tanabe Y and Kamimura H 1970 *Multiplets of Transition Metals in Crystal* (New York: Academic)
[12] Pryce M H I 1966 *Phonon* ed R W Stevenson (Edingburgh: Oliver & Boyd) pp 403–48
[13] Yamaga M, Henderson B, O'Donnell K P and Gao Y 1991 *Phys. Rev.* B **44** 4853
[14] Henderson B, Yamaga M, Gao Y and O'Donnell K P 1992 *Phys. Rev.* B **46** 652